The structure of the $[Fe(CN)_6]^{4-}$ shallow electron centre in silver chloride

1997 J. Phys.: Condens. Matter 9 3227

(http://iopscience.iop.org/0953-8984/9/15/014)

J. Phys.: Condens. Matter **9** (1997) 3227–3240. Printed in the UK PII: S0953-8984(97)78872-6

The structure of the $[Fe(CN)_6]^{4-}$ shallow electron centre in silver chloride

M T Bennebroek†, J Schmidt†, R S Eachus‡ and M T Olm‡

† Centre for the Study of Excited States of Molecules, Leiden University, PO Box 9504, NL-2300 RA Leiden, The Netherlands

‡ Imaging Research and Advanced Development, Eastman Kodak Company, Rochester, NY 14650-2021, USA

Received 23 October 1996

Abstract. The results of an ENDOR study of electrons shallowly trapped at $[Fe(CN)_6]^{4-}$ complexes doped in AgCl emulsions reveal that the dopant replaces a $[AgCl_6]^{5-}$ lattice unit without an additional lowering of the local symmetry and without the association of charge-compensating cationic vacancies. Effects of the grain structure seem to interfere in the interpretation of the results from ^{13}C-enriched $[Fe(CN)_6]^{4-}$-doped emulsions, for which an ensemble of slightly different electron centres is believed to be observed.

1. Introduction

Transition metal complexes are frequently doped into the silver halide microcrystals that constitute conventional photographic materials [1, 2]. Their function is to mediate the formation of the latent image by affecting electron and/or hole processes initiated by the absorption of actinic photons. Some complexes are particularly effective in reducing recombination inefficiencies in AgX materials sensitized to long-wavelength light by the adsorption, as crystalline aggregates, of certain red dyes [3]. This recombination is thought to occur between electrons injected into the substrate from the photo-excited dye, and holes remaining in the sensitizing aggregate. The iron group M^{2+} hexacyanides are typical examples of dopants that can overcome this dye-related inefficiency. Thus, the mechanisms by which they affect the photochemistry of the host silver halide are of both fundamental and practical interest.

Electron paramagnetic resonance (EPR) experiments performed on $[Fe(CN)_6]^{4-}$-doped silver chloride microcrystals (or grains) of uniform size and cubic morphology have been particularly informative [4, 5]. It appears that two types of centre can be distinguished: those with a charge-compensating (cation) vacancy in the close proximity of the $[Fe(CN)_6]^{4-}$ dopant and those where charge compensation results from an unassociated point defect [4, 5]. The first type gives rise to a series of $[Fe(CN)_6]^{3-}$ centres as a result of deep hole trapping during band-gap irradiation at or near to room temperature. There are at least six different hole traps, differentiated by the number and geometrical arrangement of charge-compensating silver-ion vacancies at adjacent lattice sites. These traps give characteristic EPR spectra at 10 K with anisotropic g-values, ranging from 0.6 to 3.1, and the spectra have been analysed in terms of six structural models [4, 5], assignments supported by the results of advanced computational modelling [6, 7]. All six centres decay overnight at

0953-8984/97/153227+14$19.50

room temperature, probably by hole thermalization, since the photochemistry just described is completely reversible. These EPR results are explained if, in a simple one-electron representation, the filled t_{2g} orbitals of the low-spin, $5d^6$ $[Fe(CN)_6]^{4-}$ complex lie above the valence band edge of AgCl. Since $10Dq$ is about 35 000 cm^{-1} (4.34 eV) [8], and the indirect band-gap energy of AgCl is about 3.2 eV [2], the vacant e_g orbitals of the dopant are placed at least 1.1 eV above the conduction band edge. Thus, in contrast to the situation in wide-band-gap insulators like the alkali halides [9], $[Fe(CN)_6]^{4-}$ shows no propensity to deeply trap photoelectrons in AgCl.

The second type of $[Fe(CN)_6]^{4-}$ centre in AgCl is responsible for an unexpected shallow trapping of photoelectrons observed during band-gap irradiation at low temperatures [4, 5]. This was first revealed through the detection at 20 K of a strong, isotropic EPR line centred at $g = 1.8781 \pm 0.0005$ during the continuous exposure to 365 nm light of AgCl grains nominally doped with 25 molar parts per million (mppm) of $[Fe(CN)_6]^{4-}$. By comparison to the results of earlier studies of aliovalent cationic dopants with closed-valence-shell electronic configurations, such as Pb^{2+} and Cd^{2+} [10, 11], this signal was assigned to electrons shallowly trapped at the second type of $[Fe(CN)_6]^{4-}$ centre, i.e., those that have no adjacent cation vacancy [4, 5]. Because such a complex has an excess site charge of $+1$ with respect to the silver halide host lattice, it must effectively repel photoholes whereas it can act as an ionized donor to trap electrons. The resultant centre is frequently discussed in terms of effective-mass theory as an electron precessing in a 1s-like orbital of large radius around the dopant complex [1, 2]. Thus, the shallow electron centre essentially has the properties of an electron at the conduction band edge of AgCl, and the EPR spectrum has no direct 'signature' from the dopant at the centre of the 1s-like orbital. This illustrates why no experimental proof of this model has so far been presented.

The ability of $[Fe(CN)_6]^{4-}$ dopant complexes to overcome dye-related recombination inefficiencies in photographic materials cannot be traced to their ability to trap photoholes. Since the lowest occupied molecular orbitals of the dye lie well above the silver halide valence band edge, holes are not injected into the substrate, being lost to the grain's environment over time. The ability of some $[Fe(CN)_6]^{4-}$ complexes to shallowly trap photoelectrons must be of more practical significance and, therefore, it is important to determine their structure.

Recently, it was shown that high-frequency, pulsed electron–nuclear double-resonance (ENDOR) spectroscopy can be used to obtain detailed structural information about both intrinsic and impurity-related shallow electron traps in AgCl single crystals [11]. This technique has now been applied to $[Fe(CN)_6]^{4-}$- and $[Fe(^{13}CN)_6]^{4-}$-doped AgCl photographic emulsion grains to deduce the composition and structure of the dopant-related ionized donor centre.

2. Experimental details

2.1. Materials

Dispersions in gelatin of doped silver chloride microcrystals (i.e., photographic emulsions) were prepared for this study by conventional methods [12]. The emulsion grains were cubic, with edge lengths in the range of 0.32–0.40 μm, and dopant concentrations varied between 1 and 50 molar parts per million (mppm). The dopant was dissolved in distilled water and added continuously during the growth of 4% to 70% of the grain volume. The dopant salts used were $K_4Fe(CN)_6{\cdot}3H_2O$ (Alfa Products Division of Morton Thiokol, Incorporated) and $K_3Fe(CN)_6$ (Eastman Kodak Company). $K_4Fe(^{13}CN)_6{\cdot}3H_2O$ (with labelled ^{13}C) was

prepared by reacting an aqueous solution of $FeSO_4{\cdot}7H_2O$ (Alfa) with excess $K^{13}CN$ (99.2 at.% ^{13}C, MSD Isotopes). The composition of the enriched dopant salt was verified by IR spectroscopy [13]. The emulsions were 'degelled' by centrifugation and freeze drying to obtain finely dispersed powders for EPR and ENDOR studies.

2.2. Instrumentation

The ENDOR spectra were recorded with a pulsed spectrometer operating at a microwave frequency of 95 GHz which has been described in detail elsewhere [14]. In the experiment, the samples were cooled down to 1.2 K in the dark after which no EPR signals could be observed. The EPR signal of the $g = 1.878$ shallow electron centre appeared upon ultraviolet irradiation at a magnetic field value of 3.6 T and the experiments have been performed under continuous exposure. The ENDOR spectra were obtained via the stimulated-echo (SE) pulse sequence originally introduced by Mims [15, 16]. Here a $\pi/2$–τ–$\pi/2$–T–$\pi/2$ microwave pulse sequence is applied resonantly with the EPR signal of the shallow electron centre which creates the SE signal at time τ after the third pulse. A radio frequency (rf) pulse, applied between the second and the third $\pi/2$ microwave pulses, induces nuclear transitions, and its effect can be monitored as a change of the SE intensity.

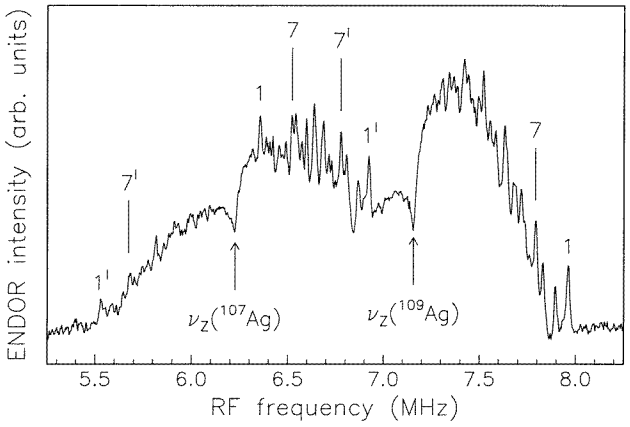

Figure 1. The silver ENDOR spectrum of the $g = 1.878$ shallow electron centre in a 5 mppm, $[Fe(CN)_6]^{4-}$-doped AgCl emulsion. This spectrum has been recorded with $\pi/2 = 90$ ns, $\tau = 400$ ns, $T = 1030$ μs, and a rf pulse length of 1020 μs. The ^{107}Ag and ^{109}Ag transitions from two inequivalent ions are labelled by their primed and unprimed (shell) numbers, respectively.

3. Results and analysis

In figure 1, the silver ENDOR spectrum of the shallow electron centre is presented; this has been recorded upon ultraviolet irradiation at 1.2 K of a $[Fe(CN)_6]^{4-}$-doped AgCl emulsion with an aim dopant concentration of 5 mppm. The spectrum contains transitions of both the ^{107}Ag ($I = \frac{1}{2}, 52\%$) and ^{109}Ag ($I = \frac{1}{2}, 48\%$) isotopes, and the positions of the corresponding nuclear Zeeman frequencies at 6.22 MHz and 7.16 MHz are indicated in the figure. As discussed previously [11, 17], each ENDOR line corresponds to the

superhyperfine (shf) interaction of the shallowly trapped electron with the silver ions that surround the Coulombic binding centre. The fact that a multitude of lines is observed indicates that the trapped electron interacts with a large number of ions and thus confirms its delocalized nature. It has been shown [11, 17] that an electron (with $S = \frac{1}{2}$) interacting with a single ion α (with nuclear spin $I_\alpha = \frac{1}{2}, 1, \frac{3}{2}, \ldots$) gives rise to two ENDOR transitions which are symmetrically placed around the nuclear Zeeman frequency $g_{n\alpha}\beta_n B_0$ according to

$$\nu_{\mathrm{ENDOR}}(M_S = \pm\tfrac{1}{2}; \alpha) = \frac{1}{h}\left|g_{n\alpha}\beta_n B_0 \mp \frac{a_\alpha}{2}\right|. \tag{1}$$

Here, only the shf interaction is included, and the quadrupole interaction for nuclei α with $I_\alpha \geqslant 1$ has been neglected. For SECs in silver halides, the shf constant a_α is isotropic as a consequence of the very diffuse nature of the trapped electron, and in fact it is this isotropic property which enables one to record the ENDOR spectrum of SECs in (powder-like) emulsions. To illustrate the symmetrical distribution given by equation (1) we marked in figure 1 the ENDOR transitions originating from two inequivalent ions α. Here the unprimed and primed numbers indicate ^{107}Ag and ^{109}Ag transitions, respectively. The latter transitions are stronger as a result of the (roughly) linear increase of the ENDOR effect in this frequency region. A remarkable feature is that the low-frequency parts of both the ^{107}Ag and ^{109}Ag spectra are about a factor of two less intense compared to their high-frequency counterparts. Since for a shallow electron interacting with a silver nucleus, the sign of a_α has been established to be negative [18], and because $g_{n\alpha}(\mathrm{Ag}) < 0$, these low- and high-frequency parts correspond to nuclear transitions in the $M_S = +\frac{1}{2}$ and $M_S = -\frac{1}{2}$ manifolds, respectively (see equation (1)). A similar intensity ratio is observed in the chlorine ENDOR spectrum containing nuclear transitions of the ^{35}Cl ($I = \frac{3}{2}$, 76%) and ^{37}Cl ($I = \frac{3}{2}$, 24%) isotopes. For chlorine, the signs of $g_{n\alpha}$ and a_α are both positive [18]. The observed intensity ratio of the ENDOR transitions in the $M_S = +\frac{1}{2}$ and $M_S = -\frac{1}{2}$ manifolds is typical for the SEC in the $[Fe(CN)_6]^{4-}$-doped AgCl emulsion, but was not observed for the other SECs in AgCl [11].

For a detailed analysis, only parts of the silver and chlorine ENDOR spectra are needed, and in figures 2(a) and 3(a) the relevant high-frequency parts of the ^{109}Ag and the ^{35}Cl ENDOR spectra are shown. These were recorded from a 5 mppm $[Fe(CN)_6]^{4-}$-doped AgCl emulsion. As is evident from equation (1), one can derive from these spectra the value of the isotropic hf interaction a_α of the shallow electron with many silver and chlorine lattice ions. Since this interaction is proportional to the spin density $|\Psi(\alpha)|^2$ on the nuclei of these ions, i.e.,

$$a_\alpha = \frac{8\pi}{3} g_e\beta_e g_{n\alpha}\beta_n |\Psi(\alpha)|^2 \tag{2}$$

it is possible to derive the spatial distribution of the spin density. The result is shown in figure 4 where the circles and triangles are derived from the ^{109}Ag and ^{35}Cl ENDOR spectra, respectively. These symbols do not reflect the 'real' spin densities $|\Psi(\alpha)|^2$ of the appropriate many-electron wave function Ψ, describing not only the unpaired shallow electron but also the core electrons of the lattice ions, but rather the densities $|\Phi(\alpha)|^2$ of the more convenient 'envelope' function Φ. This 'envelope' function gives an approximate description of the shallow electron without consideration of the nodal behaviour of its wave function within the cores of the lattice ions. It has been shown that the real spin density $|\Psi(\alpha)|^2$ is related to the approximate spin density $|\Phi(a)|^2$ via

$$|\Psi(\alpha)|^2 = A_\alpha |\Phi(\alpha)|^2 \tag{3}$$

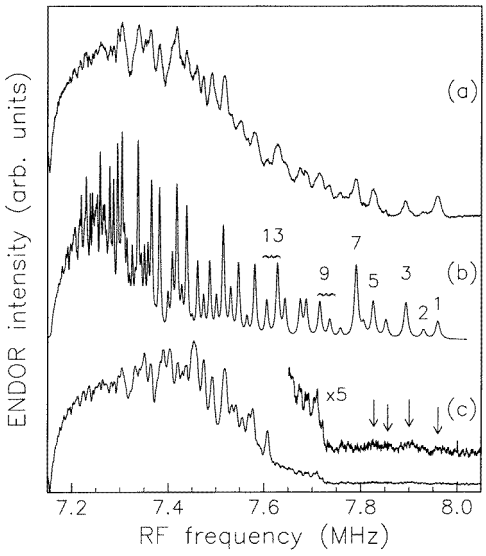

Figure 2. The high-frequency part of the ^{109}Ag ENDOR spectrum obtained for the shallow electron centre in (a) non-enriched and (c) ^{13}C-enriched $[Fe(CN)_6]^{4-}$-doped AgCl emulsions with dopant concentrations of 5 mppm. These spectra have been constructed from several narrow recordings (typical width 0.3 MHz) taken at different values of τ (ranging from 400 ns to 700 ns). (b) reflects a simulation of the ENDOR spectrum, where Lorentzians are used to represent ENDOR line-shapes and the calculated spectrum is multiplied near the ^{109}Ag nuclear Zeeman frequency at 7.16 MHz by the factor $\{1 - \cos[2\pi(\nu_{rf} - \nu_z)\,2\tau]\}$ to account for the frequency dependence of the ENDOR effect [22]. The labels indicate the shell numbers from which the transitions originate.

where the 'amplification factor' A_α in the case of a shallow electron centre only depends (to a first approximation) on the species of ion α and not on its position in the lattice [11, 17]. Figure 4 has been constructed using $A_{Ag} = 3078$ and $A_{Cl} = 1333$. These values have been derived from the silver and chlorine spectra using equations (1), (2), (3) together with the expression for the envelope function:

$$\Phi(\boldsymbol{r}) \propto \begin{cases} (1 + r/r_1)\mathrm{e}^{-r/r_1} & r \leqslant R_c \\ \mathrm{e}^{-r/r_0} & r > R_c \end{cases} \tag{4}$$

which, when normalized, is known to properly describe the radial dependence of SECs in silver halides [17]. Function (4) also gives a reasonable description of the SEC in $[Fe(CN)_6]^{4-}$-doped AgCl as illustrated by the solid line in figure 4, where we used $r_0 = 18.5$ Å, $r_1 = 12.5$ Å, and $R_c = 20$ Å. However, at radii smaller than 9.6 Å (or $r < 3.5d$ in the figure, with the interionic lattice distance $d = 2.7532$ Å) [19], a distinct deviation is observed. An explanation for this deviation will be given in the next section.

To illustrate the assignment of the ENDOR lines that led to the radial dependence shown in figure 4, we have included simulations of the high-frequency parts of the ^{109}Ag and ^{35}Cl ENDOR spectra in figures 2(b) and 3(b). For most ions located at a distance r from the centre, the ENDOR frequencies can be calculated using function (4), and the number of ions at an identical radius can be used as a measure for the ENDOR intensity. However, for the ions with $r < 9.6$ Å ($=3.5d$) the frequencies were adjusted manually to the experimental

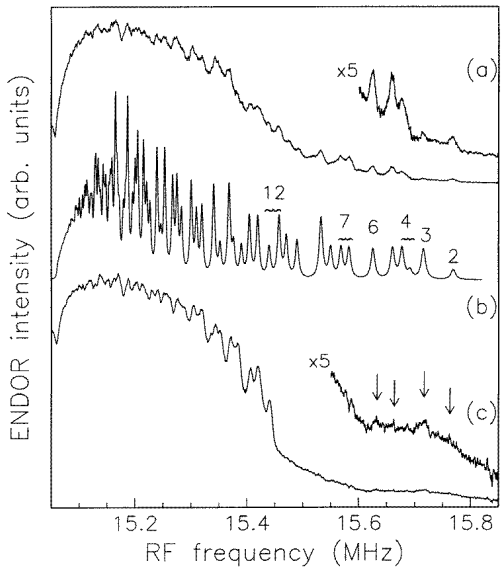

Figure 3. The high-frequency part of the ^{35}Cl ENDOR spectrum obtained for the shallow electron centre in (a) non-enriched and (c) ^{13}C-enriched $[Fe(CN)_6]^{4-}$-doped AgCl emulsions with dopant concentrations of 5 mppm. As in figure 2, these spectra have been constructed from several narrow recordings. The ^{35}Cl nuclear Zeeman frequency is positioned at 15.06 MHz. (b) reflects a simulation of the ENDOR spectrum, and the numbers label the chlorine shells from which the transitions originate.

values. Moreover, for $r < 14$ Å ($=5.1d$), ions with an identical radius but located at different symmetry positions appear to have slightly different ENDOR frequencies, as will be discussed in the next section. The spectra can only be simulated when the centre position of the envelope function is placed on a Ag^+ lattice position since for any other position the resulting patterns of line intensities do not match the experimentally observed intensity patterns. Note that no signal from the first chlorine shell, containing six ions at [100] positions, is observed.

So far, we have presented and analysed the shf data obtained from the silver and chlorine ENDOR spectra which reveal the spatial extension of the shallowly trapped electron. No direct information about the binding centre of the SEC has been obtained in the 5 mppm $[Fe(CN)_6]^{4-}$-doped emulsion because no ENDOR transitions of ^{57}Fe ($I = \frac{1}{2}$, 2% and $\nu_Z = 4.97$ MHz), ^{13}C ($I = \frac{1}{2}$, 1% and $\nu_Z = 38.66$ MHz), and ^{14}N ($I = 1$, 99.6% and $\nu_Z = 11.11$ MHz) were observed. For ^{57}Fe and ^{13}C the lack of observation is no surprise as their natural abundances are very low. The ^{14}N ENDOR lines might be hidden from detection by line broadening by the (anisotropic) quadrupole interaction in combination with the powder-like composition of the emulsion. Moreover, as the ^{14}N Zeeman frequency is located between the spectral regions of silver and chlorine, the ^{14}N transitions might be obscured by silver and chlorine transitions as well.

The nuclear transitions of ^{13}C have been observed in a ^{13}C-enriched $[Fe(CN)_6]^{4-}$-doped AgCl emulsion with a doping level of 5 mppm, and the ENDOR spectrum is shown in figure 5. The high-frequency parts of the ^{109}Ag and ^{35}Cl ENDOR spectra, obtained in this enriched emulsion, are included in figures 2(c) and 3(c) for comparison.

4. Discussion

In this section, first the ENDOR results of the non-isotopic-enriched $[Fe(CN)_6]^{4-}$-doped AgCl emulsion will be considered, which yield information about the shf interaction of the shallowly trapped electron with the silver and chlorine lattice ions. Then, we turn to the results for the ^{13}C-enriched $[Fe(CN)_6]^{4-}$-doped emulsion which are more difficult to interpret.

4.1. ENDOR for $[Fe(^{12}CN)_6]^{4-}$-doped AgCl

The analysis of the previous section reveals that the silver and chlorine ENDOR spectra can only be simulated when the electron trap is centred on a Ag^+ lattice position. For this position, the ENDOR transitions of many lattice ions can be identified even up to the 87th silver shell at 37.5 Å and the 61st chlorine shell at 34.9 Å from the centre. Since the lines of the first chlorine shell containing six ions at [100] positions are missing in the chlorine ENDOR spectrum of figure 3(a), it seems likely that the $[Fe(CN)_6]^{4-}$ dopant replaces a $[AgCl_6]^{5-}$ unit. If true, and when no charge-compensating vacancies are nearby, the introduced complex has an excess Coulombic charge of $+1$ and thus can give rise to a SEC by the capture of an electron. In the previous section, we demonstrated that at large radii ($r > R_c$) the spatial distribution of the trapped electron is described by a simple exponential function with a Bohr radius $r_0 = 18.5 \pm 1.1$ Å. The close agreement of this value with $r_0 = 15.1 \pm 0.6$ Å derived for the self-trapped exciton in AgCl [18], which is known to consist of an electron bound to a centre with an excess charge $+1$, indicates that the SEC in the $[Fe(CN)_6]^{4-}$-doped AgCl emulsion has the same Coulombic charge. This result supports the model in which a $[AgCl_6]^{5-}$ unit is replaced by $[Fe(CN)_6]^{4-}$.

The Bohr radius $r_0 = 18.5 \pm 1.1$ Å of our $[Fe(CN)_6]^{4-}$-related SEC is slightly larger than the value $r_0 = 18.2 \pm 1.1$ Å obtained for the Pb-related SEC in AgCl [17]. From uv-induced infrared absorption spectroscopy, the energy difference E_{1s-2p} between the hydrogen-like 1s and 2p states of the Pb-related SEC in AgCl has been determined to be $E_{1s-2p} = 30.5$ meV [20]. The value of E_{1s-2p} for the $[Fe(CN)_6]^{4-}$-related SEC is thus expected to be only slightly smaller. This estimate will be used in the next section.

From a previous ENDOR study it appeared that equation (4) can be used to describe the radial dependences of the envelope function of various SECs in silver halides [17]. This also applies to our $[Fe(CN)_6]^{4-}$-related SEC, as can be verified in figure 4, except for the silver and chlorine shells with $r < 3.5d$ where the derived densities deviate from the cuspless part of function (4). This unexpected deviation might be related to the lattice relaxation accompanying the replacement of a $AgCl_6$ unit by the (smaller) $Fe(CN)_6$ complex, the effect of which should be strongest for the nearest lattice ions. An additional effect is that the assumption underlying the derivation of the envelope function in figure 4, i.e., that for all silver ions $A_{Ag} = 3078$ and that for all chlorine ion $A_{Cl} = 1333$, seems not to be justified for the ions close to the centre of the SEC.

As discussed previously [17], the value of A_α for ion α can be obtained, in theory, by orthogonalization of the envelope function Φ to the wave functions of the core electrons of that ion. Because the wave functions for the Ag^+ and Cl^- ions in the AgCl crystal are not known, one can only make an estimate. By using, for instance, the wave functions of free ions, it was found that $A_{Ag} = 820$ and $A_{Cl} = 680$ [17]. These values deviate considerably from the experimentally derived values $A_{Ag} = 3078$ and $A_{Cl} = 1333$ and therefore indicate that the free-ion core orbitals are not preserved in the crystal. In fact, this is just a manifestation of the partial covalent bonding character of the AgCl lattice,

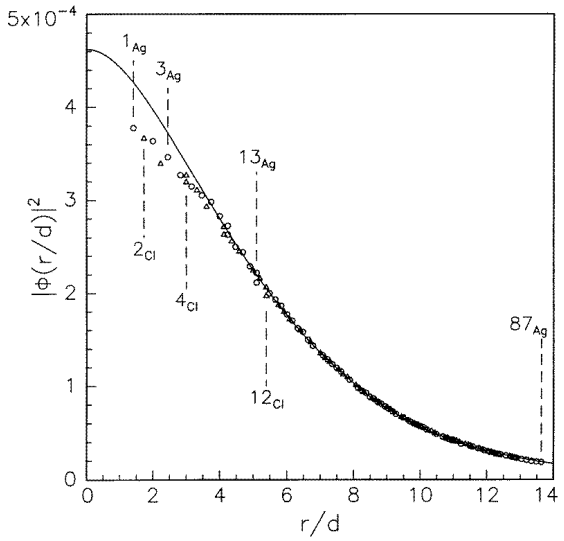

Figure 4. The density of the envelope function, derived for the shallow electron centre in the non-enriched (5 mppm) $[Fe(CN)_6]^{4-}$-doped AgCl emulsion, as a function of r/d (with $d = 2.7532$ Å, the interionic lattice distance at 0 K) [19]. The open circles and triangles denote the densities derived from the ^{109}Ag and ^{35}Cl ENDOR spectra of figures 2(a) and 3(a), respectively, and the radii of some silver and chlorine shells are indicated. The solid line reflects function (4) and the (unexpected) deviation for the experimental points with $r < 3.5d$ is discussed in section 4.1.

which means that the crystal orbitals of an ion will be affected by the neighbouring ions. Therefore, the crystal orbitals of the Ag^+ and Cl^- ions which are direct neighbours of the dopant complex can differ from those of the more remote lattice ions and, consequently, their amplification factors can be different as well. Assuming that the cuspless part of equation (4) still properly describes the radial dependence in the close proximity of the $[Fe(CN)_6]^{4-}$ complex, the deviation observed in figure 4 indicates that A_{Ag} and A_{Cl} decrease at small values of r. For example, we find for the first few silver shells at $r = 1.4d, r = 2d$, and $r = 2.4d$ that $A_{Ag}^{[110]} = 2726$, $A_{Ag}^{[200]} = 2815$, and $A_{Ag}^{[211]} = 2862$, and for the chlorine shells at $r = 1.7d$, and $r = 2.2d$ that $A_{Cl}^{[111]} = 1187$, and $A_{Cl}^{[210]} = 1175$, respectively.

When the introduction of the dopant complex does not perturb the crystal structure, all ions within a single shell would be equivalent and should contribute to a single ENDOR transition. However, the ENDOR spectra reflect that within some shells a small inequivalence exists between the constituting ions, indicating that the dopant complex is indeed accompanied by a lattice relaxation. For instance, in the ^{109}Ag ENDOR spectrum of figure 2(a), the transition of the 9th silver shell (at $r = \sqrt{18}d$), containing 24 ions at [411] and 12 ions at [330] positions, is split in two lines with a separation of 20 kHz and an intensity ratio of 2:1. The lines at 7.606 MHz and 7.628 MHz with an intensity ratio of 1:2 are attributed to the 24 ions at [510] and the 48 ions at [431] positions, which all belong to the 13th silver shell (at $r = \sqrt{26}d$). For chlorine, the 6 ions at [300] and 24 ions at [221] of the 4th chlorine shell (at $r = 3d$) are believed to be responsible for the asymmetric line-shape at 15.8 MHz in figure 3(a) whereas the two lines of equal intensity at 15.568 MHz and 15.584 MHz are ascribed to the 7th chlorine shell (at $r = \sqrt{17}d$), consisting of 24 ions at

[410] and 24 ions at [322] positions. These examples indicate that the inequivalences only occur for shells which contain two groups of ions, with similar radii r but each at a different symmetry position. This suggests that, because the lattice relaxation leaves ions at identical symmetry positions equivalent, the cubic (lattice) symmetry is maintained. If the local symmetry were to be lower than that of the lattice, ions at an identical symmetry position could also become inequivalent. For instance, the 12 silver ions at [110] are equivalent under the O_h symmetry of the lattice, but for D_{4h} symmetry they split into two groups containing 4 and 8 equivalent ions each. No such signs of a lowered local symmetry can be found in the spectra of figures 2(a) and 3(a). Therefore, we conclude that the local symmetry is cubic which, together with the excess Coulombic charge of $+1$ and the cationic-centre position of the SEC, suggests that the $[Fe(CN)_6]^{4-}$ complex replaces a $[AgCl_6]^{5-}$ unit, i.e., there is no charge-compensating silver-ion vacancy in the vicinity of the dopant.

4.2. ENDOR for ^{13}C-enriched $[Fe(CN)_6]^{4-}$-doped AgCl

In order to test the hypothesis that the $[Fe(CN)_6]^{4-}$ complex is preserved during the preparation of the doped emulsions and that it replaces a $[AgCl_6]^{5-}$ unit without lowering the cubic lattice symmetry, we performed an ENDOR study on a ^{13}C-enriched AgCl:$[Fe(CN)_6]^{4-}$ emulsion with a dopant concentration of 5 mppm. When the local symmetry is cubic, all carbon atoms in the six CN^- ligands are equivalent and should contribute to just two transitions symmetrically placed around the nuclear Zeeman frequency (see equation (1)). However, the recorded ^{13}C ENDOR spectrum is not that simple as can be seen in figure 5. It contains two relatively intense lines centred at around the ^{13}C Zeeman frequency at $\nu_Z(^{13}C) = 38.66$ MHz. The low-frequency line is split into two components with a frequency difference of 15 kHz and its intensity is about half that of its high-frequency counterpart. Moreover, in total five weak satellite lines are observed on the high-frequency side, of which only three counterparts can be resolved on the (lower-intensity) low-frequency side.

Let us first focus on the high-frequency part of the ^{13}C ENDOR spectrum shown in figure 5, which suggests that several types of SEC are present in the ^{13}C emulsion. The single, intense line closest to the ^{13}C Zeeman frequency originates from the most abundant type, which we tentatively assume to be identical to the one described above, i.e., an electron shallowly trapped at a cubic $[Fe(^{13}CN)_6]^{4-}$ complex. Judging from the line intensities, some 20% to 30% of the total SECs contribute to the low-intensity satellite transitions. Because these additional resonances take place at higher frequencies, which according to equations (1) and (2) implies that higher spin densities are involved, this suggests that roughly one quarter of the SECs in the emulsion comprise more strongly localized electrons. Support for the presence of an ensemble of SECs comes from the ^{109}Ag and ^{35}Cl ENDOR spectra shown in figures 2(c) and 3(c), respectively, which appear to consist of a superposition of several spectra. The effect of small differences in electronic distribution should be largest for the resonances of the ions near to the Coulombic core, as is evident from the observed low spectral resolution in the regions above 7.7 MHz in figure 2(c) and 15.45 MHz in figure 3(c). Because these spectra still show similarities with the ones of the non-enriched emulsion depicted in figures 2(a) and 3(a), it seems justified to assume that cubic $[Fe(^{13}CN)_6]^{4-}$ complexes are present in the ^{13}C-enriched emulsion as well. The small increase of the EPR linewidth from $(24.0 \pm 0.5) \times 10^{-4}$ T for the non-enriched emulsion to $(25.3 \pm 0.6) \times 10^{-4}$ T for the ^{13}C-enriched emulsion, both with a dopant concentration of 5 mppm, supports the contention that some of the SECs in the latter sample are related to (slightly) more deeply trapped electrons.

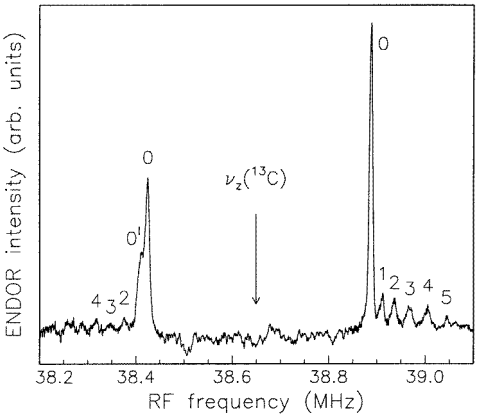

Figure 5. The ^{13}C ENDOR spectrum recorded in a ^{13}C-enriched $[Fe(CN)_6]^{4-}$-doped AgCl emulsion with a dopant concentration of 5 mppm. The ^{13}C nuclear Zeeman frequency is positioned at 38.66 MHz. The interpretation of this spectrum is discussed in section 4.2.

A possible interpretation of the high-frequency part of the ^{13}C ENDOR spectrum might be that a distribution of $[Fe(^{13}CN)_{6-x}L_x]^{4-}$ complexes is present in the ^{13}C-enriched emulsion, where x ranges from 0 to 6 and L denotes Cl^- (or perhaps H_2O introduced during precipitation into the grain). The line closest to the ^{13}C Zeeman frequency is then ascribed to the complex with $x = 0$, whereas the weak satellite lines are subsequently assigned to complexes where one or more of the CN^- ligands are replaced. This interpretation implies that the imperfect complexes give rise to more strongly localized SECs, which is in line with the observation that the upper value of the transition energy E_{1s-2p} of 30.5 meV estimated in the previous section for the $[Fe(^{12}CN)_6]^{4-}$-related SEC (in which none of the CN^- ligands are replaced) is lower than the reported value $E_{1s-2p} = 32.8$ meV for the $[FeCl_6]^{4-}$-related SEC in AgCl single crystals [20] (in which all CN^- ligands are replaced by Cl^-). However, we tend to rule out this interpretation for two reasons. First, cyanide is a strong ligand for iron and it is highly unlikely that one or more CN^- ions will be replaced under the mild chemical conditions chosen during the preparation of the emulsions. Moreover, exposure of $[Fe(CN)_6]^{4-}$-doped AgCl grains to chlorine gas at 250 K is known to produce a series of $[Fe(CN)_6]^{3-}\cdot n$V paramagnetic centres, i.e., complexes of Fe^{3+} surrounded by six CN^- ligands and accompanied by $n = 0$, 1, 2 silver-ion vacancies [4, 5]. The strongly localized spin of such d^5-like complexes makes them very sensitive to the symmetry and distortions of their surrounding. After chemical oxidation with Cl_2 of the ^{13}C-enriched sample used in the ENDOR experiments, only the signals belonging to the $[Fe(CN)_6]^{3-}\cdot n$V centres show up. This indicates that for most of the $[Fe(CN)_6]^{4-}$ complexes doped into the grains, the six iron–cyanide bonds must be preserved.

It seems not likely that the observed multiplet structure in the ^{13}C, ^{109}Ag and ^{35}Cl ENDOR spectra can be attributed to complexes with mixtures of $^{12}CN^-$ and $^{13}CN^-$ ligands. Since we are dealing with shallow electrons which possess a very low density at the Coulombic binding core, the effect of such admixtures should be very small. Moreover, the 99.2% ^{13}C enrichment cannot account for the estimated 20% to 30% of different SECs.

We suggest that the unassigned high-frequency ^{13}C ENDOR lines, labelled 1 to 5 in figure 5, result from differences in the microscopic environment of the $[Fe(^{13}CN)_6]^{4-}$ complexes caused by their location in the AgCl grain. Although the dopant was added

continuously throughout the precipitation of the emulsion, it cannot be assumed that it was introduced homogeneously. Local regions of higher dopant concentration are possible, caused by the segregation at surfaces or along grain dislocations. The trapping depth of electrons bound to such segregates is likely to differ from that of electrons shallowly trapped at isolated dopants. The association of dopants with lattice dislocations or impurities will lead to further, different perturbations of the ENDOR spectra. Also, SECs formed near to the surface of the grain will be more strongly perturbed by the negative surface charge and adsorbed ions than those at centres buried deep within the grain.

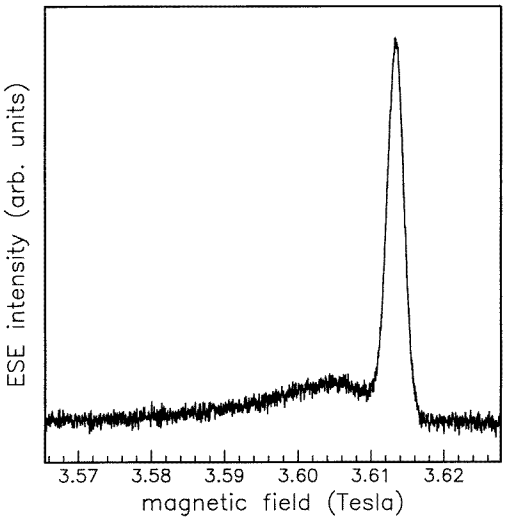

Figure 6. The ESE-detected EPR spectrum of the SEC in a ^{13}C-enriched $[Fe(CN)_6]^{4-}$-doped AgCl emulsion, recorded at 95 GHz and 1.2 K during ultraviolet irradiation. The spectrum is obtained by monitoring the intensity of the electron-spin-echo (ESE) signal created at time τ after a $\pi/2$–τ–π microwave pulse sequence as a function of the magnetic field (settings: $\tau = 500$ ns, $\pi/2$ pulse duration $= 100$ ns, and repetition rate $= 33$ Hz). The low-intensity line (at $g = 1.883$) possesses a short spin-dephasing time compared to the ($g = 1.878$) high-field one, though no quantitative study has been made. The spectrum shown is obtained from a 1 mppm doped emulsion for which the same ENDOR features are observed as in the 5 mppm sample discussed in the text, but for which the additional low-field line is more pronounced.

Circumstantial evidence supporting the latter contention comes from the EPR spectrum obtained from a ^{13}C-enriched $[Fe(CN)_6]^{4-}$-doped emulsion and shown in figure 6. In the spectrum, a low-intensity signal is observed in addition to the usual SEC signal, at a magnetic field of 3.613 T ($g = 1.878$). Because the additional peak is positioned at a lower magnetic field, and thus at a higher g-value ($g = 1.883$), it indicates the presence of (slightly) more deeply trapped SEC species, which is in agreement with the conclusion reached above. Since such additional EPR signals have not been observed for any of the SECs studied by us so far in crystals, they might be related to surface effects. Some caution should be exercised, because in the case of the non-enriched emulsion discussed in section 4.2, no such effects have been observed in both EPR and ENDOR for the SECs, whereas the grain size in this emulsion has the same dimensions as the ^{13}C-enriched grains. Apparently, the preparation conditions are of crucial importance. In order to sort out the role of the surface, it seems useful to study the dependence of the EPR lineshape of $[Fe(CN)_6]^{4-}$-doped

emulsions, prepared under identical conditions, on the grain size.

Turning to the low-frequency part of figure 5, only three of the five satellite lines are found, owing to the low intensity of this part of the spectrum and to the splitting of the intense line into two components 0 and 0′. It is interesting to note that a similar intensity ratio is present in the ENDOR spectrum of silver (see figure 1) where the low-intensity transitions are related to the $M_S = +\frac{1}{2}$ manifold (see section 3). Assuming that the weak ^{13}C ENDOR transitions originate from the same M_S-manifold, equation (1) (with $g_n(^{13}\mathrm{C})$ positive) yields that the hf interaction of the shallowly trapped electron with ^{13}C is positive. The nature of the splitting of 15 kHz between the low-frequency lines 0 and 0′ is unclear. In principle, the observed intensity ratio suggests that the six ^{13}C atoms are inequivalent and can be divided into two groups containing two and four equivalent atoms each. However, this inequivalence should manifest itself in the high-frequency counterpart, which it does not. Also the dipole–dipole interaction between the ^{13}C and ^{14}N atoms of the cyanide ligand is believed to be too small to account for the observed splitting. Using a C≡N distance of 1.16 Å, we estimate this interaction to amount to about 1.4 kHz which is ten times lower than the observed splitting. Moreover, the dipole–dipole interaction in a first-order approximation also should lead to a symmetrical pattern around the ^{13}C Zeeman frequency, which is not observed.

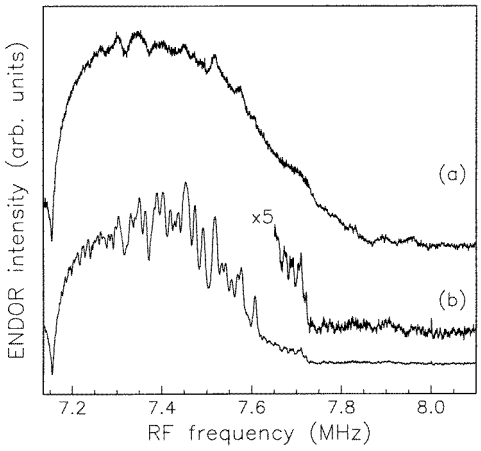

Figure 7. A comparison of the high-frequency part of the ^{109}Ag ENDOR spectrum obtained for a 50 mppm $[Fe(CN)_6]^{4-}$-doped AgCl emulsion (curve (a)) and for the 5 mppm ^{13}C-enriched $[Fe(CN)_6]^{4-}$-doped AgCl emulsion (curve (b)), shown already in figure 2(c). The similarity suggests that in the 50 mppm sample a distribution of the microscopic environments of the SECs is present, just like in the 5 mppm ^{13}C-enriched emulsion.

We note that the ENDOR spectra of figures 2 and 3 have been obtained in 5 mppm doped emulsions. We also performed experiments on a $Fe(^{12}CN)_6$-doped emulsion with a dopant concentration of 50 mppm, and the results suggest that already at this doping level an impurity band is formed due to the overlap of the extended orbitals of the SECs. In figure 7(a), the high-frequency part of the ^{109}Ag ENDOR spectrum of the 50 mppm emulsion is shown, which strongly resembles that of the 5 mppm $Fe(^{13}CN)_6$-doped emulsion, shown already in figure 2(c) and repeated in figure 7(b). Though the two spectra in figure 7 have been recorded under similar experimental conditions, it is clear that the lines in the 50 mppm emulsion are broadened compared to those in the 5 mppm emulsion. This

suggests that in the 50 mppm doped emulsion, the lifetime of an electron at one centre is shortened by a hopping process. The formation of the impurity band is supported by the reduction in EPR linewidth measured at 1.2 K from $(25.3 \pm 0.6) \times 10^{-4}$ T for the 5 mppm sample to $(22.6 \pm 0.5) \times 10^{-4}$ T for the 50 mppm emulsion, and by the results of recent photoconductivity experiments [21].

5. Conclusions

The silver and chlorine ENDOR data from electrons trapped at $[Fe(CN)_6]^{4-}$ centres in AgCl emulsions reveal that the dopant complex replaces $[AgCl_6]^{5-}$. The cubic symmetry derived for the corresponding SEC in the non-isotopically enriched 5 mppm doped emulsion is taken as confirmation of an earlier hypothesis [4, 5] that most, if not all, of the $[Fe(CN)_6]^{4-}$ dopant remains uncompensated by neighbouring silver-ion vacancies in the emulsion grain. As a consequence, the dopant has a unit positive charge with respect to the host lattice and acts as a shallow trap for electrons. This conclusion is supported by the experimentally derived Bohr radius for the SEC of 18.5 ± 1.1 Å, which is only slightly larger than that reported for the Pb^{2+}-related SEC in AgCl [17]. The deviation from the usual cuspless envelope function in the region near to the $[Fe(CN)_6]^{4-}$ dopant is attributed to the covalent nature of the AgCl lattice. This modifies the values of A_α for adjacent lattice ions with respect to their more remote counterparts.

Two features in the ^{13}C ENDOR spectrum from shallowly trapped electrons in ^{13}C-enriched $[Fe(CN)_6]^{4-}$-doped emulsions deserve further attention. The first concerns the observation of a 15 kHz splitting in the intense low-frequency ^{13}C transition, the nature of which is unclear. The second concerns the observation of weak satellite lines accompanying the main low- and high-frequency ^{13}C transitions. At present, the most probable explanation seems to be that a distribution of the microscopic environments of the SECs is present in this emulsion, which affects the spatial extent of the shallowly trapped electrons monitored in the experiment. This is supported by the apparent multiplet structure in the ^{109}Ag and ^{35}Cl shf ENDOR spectra. Possibilities include surface effects, weak associations with impurities and/or with far-distant silver-ion vacancies, and structural inhomogeneities introduced in the microscopic grains during precipitation. Further experiments are required to clarify this situation, for instance by studying the role of surface effects

Acknowledgments

We wish to thank Dr W G McDugle for preparing ^{13}C-enriched $K_4[Fe(CN)_6]$ for these studies, and Dr O G Poluektov and A Arnold for experimental assistance in the ENDOR experiments.

References

[1] Eachus R S and Olm M T 1989 *Annu. Rep. Prog. Chem.* **86** 3
[2] Marchetti A P and Eachus R S 1992 *Adv. Photochem.* **17** 145
[3] Bell E L, Reed K J and Olm M T 1992 *US Patent No* 5132203
[4] Olm M T, Eachus R S and McDugle W G 1993 *Bulg. Chem. Commun.* **26** 350
[5] Olm M T and Eachus R S 1995 *Radiat. Eff. Defects Solids* **135** 101
[6] Baetzold R C and Eachus R S 1996 *Int. Conf. on Defects in Insulating Materials (Winston-Salem, NC)*
[7] Baetzold R C 1997 *J. Phys. Chem.* at press
[8] Jørgensen C K 1962 *Absorption Spectra and Chemical Bonding in Complexes* (Oxford: Pergamon)
[9] Root K D J and Symons M C R 1983 *Radiat. Eff. Defects Solids* **73** 69

[10] Eachus R S and Spoonhower J P 1982 *Photogr. Sci. Eng.* **26** 20
[11] Bennebroek M T, Poluektov O G, Zakrzewski A J, Baranov P G and Schmidt J 1995 *Phys. Rev. Lett.* **74** 442
[12] See, for example,
James T H (ed) 1977 *The Theory of the Photographic Process* 4th edn (New York: Macmillan)
[13] Nakamoto K 1986 *Infrared and Raman Spectra of Inorganic and Coordination Compounds* 4th edn (New York: Wiley)
[14] Disselhorst J A J M, van der Meer H, Poluektov O G and Schmidt J 1995 *J. Magn. Reson.* A **115** 183
[15] Mims W B 1965 *Proc. R. Soc.* A 283
[16] Mims W B 1972 *Electron Paramagnetic Resonance* ed S Geschwind (New York: Plenum)
[17] Bennebroek M T, Arnold A, Poluektov O G, Baranov P G and Schmidt J 1996 *Phys. Rev.* B **54** 11 276
[18] Bennebroek M T, Arnold A, Poluektov O G, Baranov P G and Schmidt J 1996 *Phys. Rev.* B **53** 15 607
[19] Corish J and Fitzsimons P B 1987 *Phil. Mag.* A **56** 1
[20] Sakuragi S and Kanzaki H 1977 *Phys. Rev. Lett.* **38** 1302
[21] Eachus R S and Olm M T 1995 *10th Int. Conf. on Dynamical Processes in Excited States of Solids (Cairns, Australia)*
[22] Gemperle C and Schweiger A 1991 *Chem. Rev.* **91** 1481